Electronic supplementary information

A (3, 4, 14)-connected framework with various distorted triangular magnetic lattices exhibiting field-induced metamagnetism, spin competition and spin reorientation

Zhong-Yi Liu, Bo Ding, En-Cui Yang* and Xiao-Jun Zhao*

Synthesis of 1

A mixture containing Htrz (28.0 mg, 0.4 mmol), NaH_2sip (54.0 mg, 0.2 mmol), $Co(NO_3)_2 \cdot 6H_2O$ (148.0 mg, 0.3 mmol) was dissolved in mixed H_2O–C_2H_5OH medium (v:v = 1:1, 10.0 mL) with constant stirring. The initial pH value of the mixture was adjusted to ca. 6.0 by triethylamine. The mixture was then transferred into a parr Teflon-lined stainless steel vessel (23.0 mL) and heated to 165 ^oC for 72 h under autogenous pressure. After the mixture was cooled to room temperature at a rate of 2.9 $^oC\ h^{-1}$, pink block-shaped crystals suitable for X-ray analysis were generated directly, washed with ethanol, and dried in air. Yield: 43% based on NaH_2sip. Anal. Calcd for $C_{16}H_{18}Co_{3.5}N_{12}O_{10.5}S$: C 24.49, H 2.31, N 21.42%. Found: C 24.66, H, 2.17, N 21.53%. IR (KBr, cm^{-1}): 3421(s), 3145(w), 1615(s), 1544(s), 1504(s), 1368(s), 1272(w), 1210(m), 1147(m), 1054(m), 996(w), 662(w), 622(m).

Crystal data: $C_{16}H_{18}Co_{3.5}N_{12}O_{10.5}S$, *M*r = 784.74, monoclinic, $P2_1/n$, a = 14.143(2), b = 12.699(2), c = 15.039(3) Å, β = 96.866(3)°, V = 2681.5(8) Å^3, Z = 4, *D*c = 1.944 g cm^{-3}, μ = 2.288 mm^{-1}, F (000) = 1570, GOF = 1.040, a total of 13308 reflections were collected, 4714 of which were unique (R_{int} = 0.0659). R_1 (wR_2) = 0.0353 (0.0691) ($I > 2\sigma(I)$). $R_1(wR_2)$ = 0.0592 (0.0758) (all data). Data were collected on a Bruker APEX-II QUAZAR CCD diffractometer equipped with graphite-monochromated Mo-Ka radiation (λ = 0.71073 Å) at 296(2) K. The SADABS program was used for the absorption correction. All structures were solved by direct methods and refined on F^2 by full-matrix least-squares methods using the SHELX97 program package.

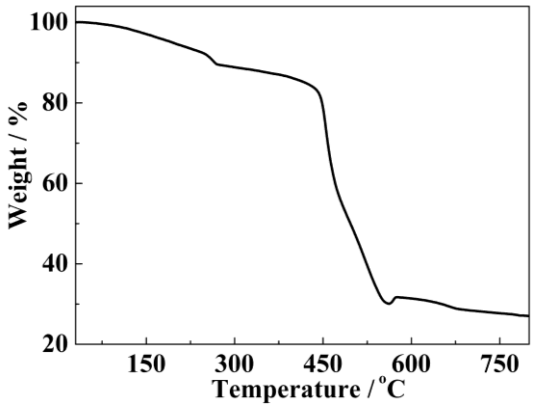

Fig. S1. TG curve for **1**.

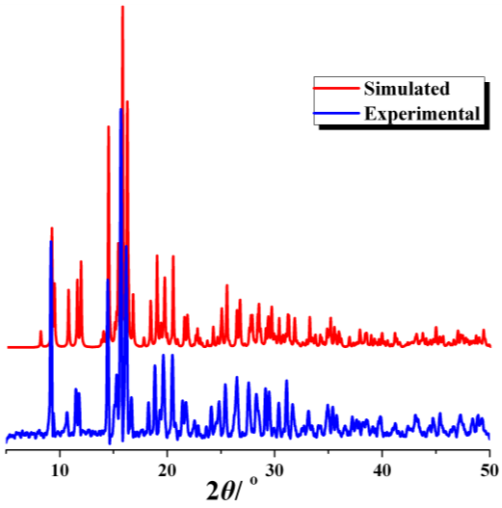

Fig. S2. Simulated (red) and experimental (blue) PXRD patterns for **1**.

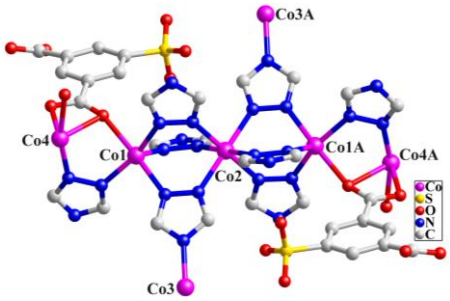

Fig. S3. The fundamental structural unit of **1**.

Table S1. Selected bond distance (Å) and angles (°)

Co(1)–N(11)	2.021(3)	Co(1)–N(4)	2.021(3)
Co(1)–N(1)	2.065(3)	Co(1)–N(7)	2.103(3)
Co(1)–O(2)	2.182(2)	Co(2)–N(5)	2.092(2)
Co(2)–N(2)	2.204(3)	Co(2)–N(8)	2.114(3)
Co(3)–N(9)	2.019(3)	Co(3)–O(5)$^{\#3}$	2.195(2)
Co(3)–N(12)$^{\#2}$	2.029(3)	Co(3)–N(3)$^{\#3}$	2.057(3)
Co(3)–O(9)	2.082(2)	Co(4)–O(2)	2.297(2)
Co(4)–O(4)$^{\#3}$	1.994(3)	Co(4)–N(6)$^{\#4}$	2.013(3)
Co(4)–O(1)	2.026(3)	Co(4)–N(10)	2.109(3)
Co(4)–O(8)	2.177(2)		
N(11)–Co(1)–N(4)	161.62(10)	N(11)–Co(1)–N(1)	98.84(12)
N(4)–Co(1)–N(1)	98.18(12)	N(11)–Co(1)–N(7)	93.74(12)
N(4)–Co(1)–N(7)	92.27(12)	N(1)–Co(1)–N(7)	92.88(11)
N(11)–Co(1)–O(2)	85.87(11)	N(4)–Co(1)–O(2)	86.05(10)
N(1)–Co(1)–O(2)	94.15(10)	N(7)–Co(1)–O(2)	172.93(10)
N(5)$^{\#1}$–Co(2)–N(5)	180.00(12)	N(5)$^{\#1}$–Co(2)–N(8)$^{\#1}$	88.11(11)
N(5)–Co(2)–N(8)$^{\#1}$	91.89(11)	N(5)$^{\#1}$–Co(2)–N(8)	91.89(11)
N(5)–Co(2)–N(8)	88.11(11)	N(8)$^{\#1}$–Co(2)–N(8)	180.0
N(5)$^{\#1}$–Co(2)–N(2)	88.13(10)	N(5)–Co(2)–N(2)	91.87(10)
N(8)$^{\#1}$–Co(2)–N(2)	88.99(12)	N(8)–Co(2)–N(2)	91.01(12)
N(5)$^{\#1}$–Co(2)–N(2)$^{\#1}$	91.87(10)	N(5)–Co(2)–N(2)$^{\#1}$	88.13(10)
N(8)$^{\#1}$–Co(2)–N(2)$^{\#1}$	91.01(12)	N(8)–Co(2)–N(2)$^{\#1}$	88.99(12)
N(2)–Co(2)–N(2)$^{\#1}$	180.0	N(9)–Co(3)–N(12)$^{\#2}$	109.74(12)
N(9)–Co(3)–N(3)$^{\#3}$	120.43(12)	N(12)$^{\#2}$–Co(3)–N(3)$^{\#3}$	128.62(13)
N(9)–Co(3)–O(9)	96.94(11)	N(12)$^{\#2}$–Co(3)–O(9)	91.55(10)
N(3)$^{\#3}$–Co(3)–O(9)	92.76(11)	N(9)–Co(3)–O(5)$^{\#3}$	85.98(11)
N(12)$^{\#2}$–Co(3)–O(5)$^{\#3}$	84.61(10)	N(3)$^{\#3}$–Co(3)–O(5)$^{\#3}$	88.33(11)
O(9)–Co(3)–O(5)$^{\#3}$	175.80(10)	O(4)$^{\#3}$–Co(4)–N(6)$^{\#4}$	102.22(12)
O(4)$^{\#3}$–Co(4)–O(1)	152.42(11)	N(6)$^{\#4}$–Co(4)–O(1)	104.26(11)
O(4)$^{\#3}$–Co(4)–N(10)	87.57(11)	N(6)$^{\#4}$–Co(4)–N(10)	101.98(12)
O(1)–Co(4)–N(10)	94.36(11)	O(4)$^{\#3}$–Co(4)–O(8)	87.36(10)
N(6)$^{\#4}$–Co(4)–O(8)	93.14(10)	O(1)–Co(4)–O(8)	83.64(10)
N(10)–Co(4)–O(8)	164.75(10)	O(4)$^{\#3}$–Co(4)–O(2)	92.37(10)
N(6)$^{\#4}$–Co(4)–O(2)	164.75(11)	O(1)–Co(4)–O(2)	60.73(9)
N(10)–Co(4)–O(2)	82.86(10)	O(8)–Co(4)–O(2)	83.00(9)

Symmetry codes: $^{\#1}$ $1-x, 1-y, -z$; $^{\#2}$ $1-x, 2-y, -z$, $^{\#3}$ $x-1/2, 3/2-y, z-1/2$; $^{\#4}$ $1/2-x, y+1/2, 1/2-z$.

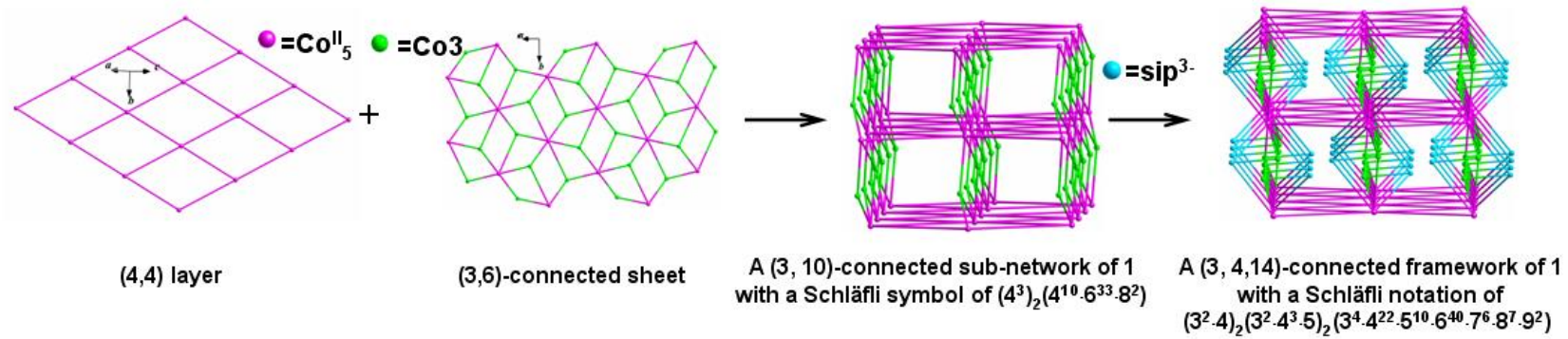

Fig. S4. Topological analyses of the 3D sub-framework and overall network of **1**.

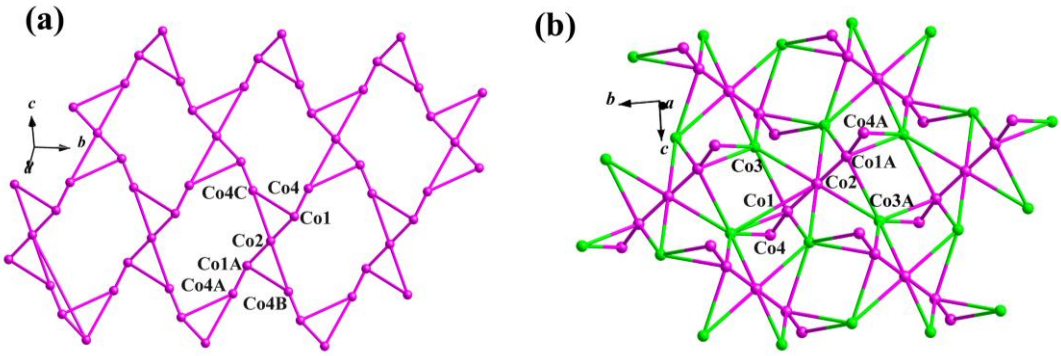

Fig. S5. The distorted triangular magnetic lattices in (4, 4) and 3, 6-connected layers.

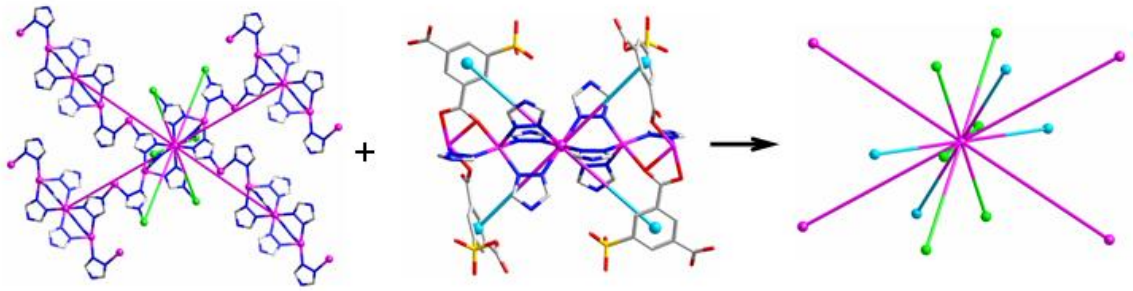

(a)

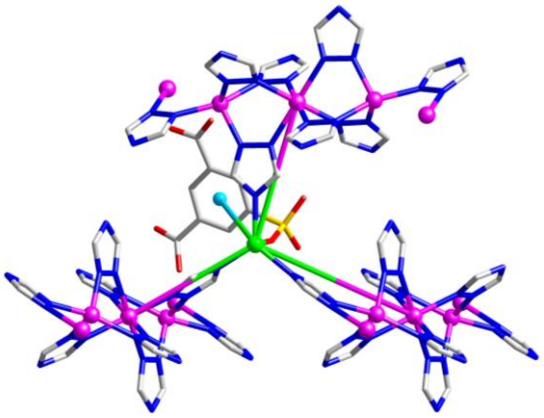

(b)

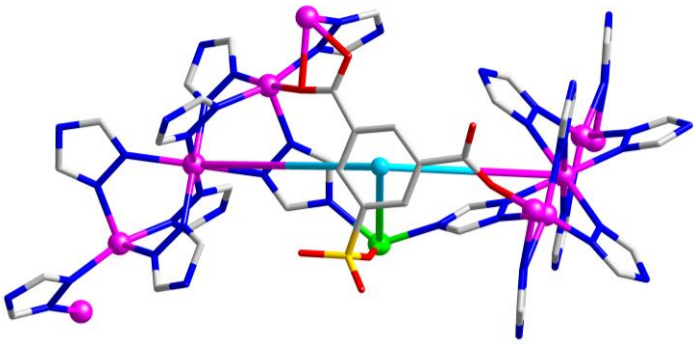

(c)

Fig. S6 (a) 14-connected Co^{II}_5 core. (b) 4-connected Co3 ion. (c) 3-connected sip^{3-} ligand.

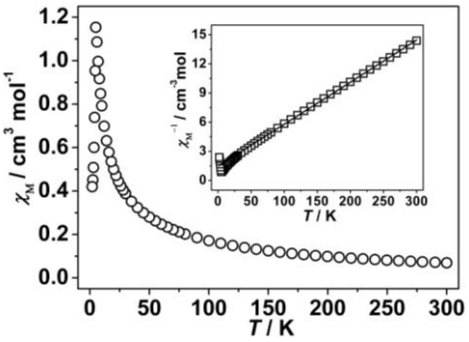

Fig. S7. Temperature dependence of χ_M for **1** (The solid line represents the best fit to Curie–Weiss law).

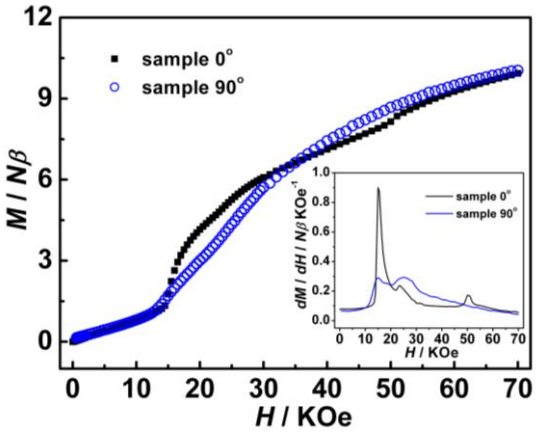

Fig. S8. The plots of *M vs H* for the polycrystalline sample of **1** in the direction of parallel and perpendicular to the horizontal axis, respectively.

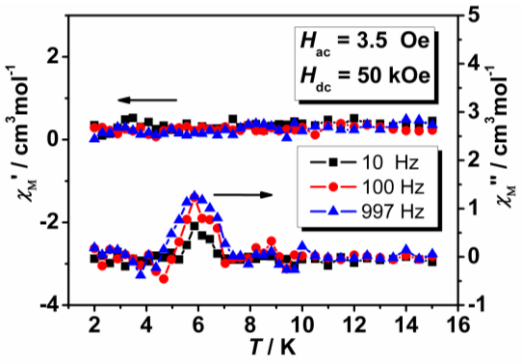

Fig. S9. Temperature dependence of ac magnetic susceptibilities of **1** in 50.0 kOe with an oscillating field of 3.5 Oe at various frequencies.

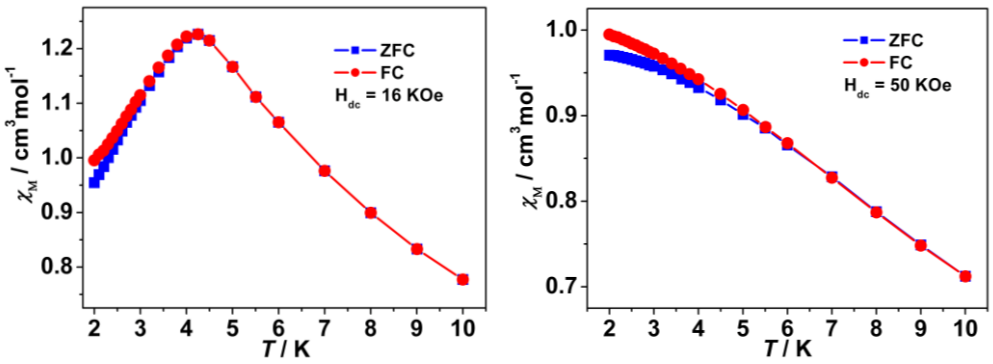

Fig. S10. The FC and ZFC magnetizations for **1** at 16 kOe and 50 kOe, respectively.